

Spectra of molecular gases trapped in deep optical lattices

P. F. Barker and S. M. Purcell

Department of Physics and Astronomy, University College London, WC1E 6BT, United Kingdom

M. N. Shneider

Department of Mechanical and Aerospace Engineering, Princeton University, Princeton, New Jersey 08544, USA

(Received 30 March 2008; published 9 June 2008)

We study the spectral profile of Rayleigh scattered light from molecular species trapped in optical lattices created by strong fields in the 10^{16} W m⁻² range. We show that, for lattices with well depths on the order of 100 K, the motional sidebands imparted on spectra are shifted from the central Dicke-narrowed Rayleigh peak by hundreds of MHz. Our calculations for these short duration (30 ns) lattices show that these spectral features appear even in room temperature gases suggesting a new technique for measuring gas composition based on the frequency offset of the sidebands. Finally, we study the role of field-induced molecular alignment within the lattice and calculate its effect on the shape and position of the sidebands.

DOI: [10.1103/PhysRevA.77.063409](https://doi.org/10.1103/PhysRevA.77.063409)

PACS number(s): 37.10.Vz, 33.70.Jg, 37.10.Pq

I. INTRODUCTION

The confinement of atomic and molecular gases to spatial scales comparable to the wavelength of light leads to sub-Doppler linewidths via the Dicke effect [1]. Such narrow-bandwidth spectral features have been observed in atoms and molecules in the optical [2], infrared [3], and microwave region [4], where the mean free path of the emitter is comparable to the wavelength of light. Such a situation can occur, for example, by confinement in a buffer gas for the optical and infrared regime or by the walls of the gas vessel for the microwave regime. A similar process results in the narrowing of x-ray spectra via the Mössbauer effect [5]. In this case the momentum due to recoil following emission of a high energy photon is taken up by the lattice of the crystal structure. In all cases the momentum of the absorber or emitter is transferred to its environment so that the momentum and thus the motional Doppler shift is reduced or eliminated.

Externally applied fields can also tightly confine atoms and molecules to spatial scales comparable to the absorbed or emitted wavelength such that their spectra are Dicke narrowed. This was predicted some time ago by Letokhov *et al.* for atoms confined to a standing wave field [6]. These features have been observed in the spectra of cold atoms or ions confined by an externally applied optical or electrostatic potential [7–9]. Such cold species can be deeply bound in even relatively weak potentials in the μ K to mK range. As these species are bound within nearly harmonic potentials, they have the familiar central elastic scattered narrow peak that is Dicke narrowed due to confinement, while a second spectral feature results from the oscillatory motion of the particles within the potential. These oscillations produce two or more sidebands separated from the central Rayleigh peak, shifted by multiples of the primary vibrational frequency. These features can also be described by Raman transitions between quantized vibrational levels within the potential. The spectra of cold atoms trapped in these types of optical potentials, which are created by the interference of two or more light fields (optical lattices), has been well studied. In these relatively weak (1 mK) potentials oscillation frequencies in the 100 kHz range are observed, and such shifts in frequency

from the Rayleigh peak can be measured accurately using heterodyne techniques in absorption and by Bragg scattering of a probe beam from the periodic arrangement of atoms in the lattice [10,11]. The measurement of these spectral profiles has been used to determine temperature and to study lattice dynamics. In addition, the quantized nature of the energy levels has been utilized for dissipative Raman sideband cooling of the atoms trapped in the lattice [12].

Recently we have studied the motion of molecules and atoms in deep optical lattice potentials that are 10^4 – 10^6 deeper than are typically used to confine ultracold atoms. These 10–1000 K deep potentials are produced by pulsed light fields in the 10^{16} W m⁻² range and are deep enough to manipulate even room temperature atomic and molecular gases. The large optical forces that result have also been used to slow cold (1 K) molecules in a molecular beam where the deceleration results from the molecules undergoing a half oscillation within the wells of the optical lattice [13]. Bragg scattered light from room temperature (295 K) gases that are briefly trapped in the lattice has also been measured as a function of lattice velocity [14]. This technique, called coherent Rayleigh scattering, has been used to measure temperature in flames and in weakly ionized gases. When a significant fraction of the gas is trapped by the lattice, a narrowing of the coherent Rayleigh scattering signal has been observed and indicates confinement of the atoms. This scheme was, however, not sensitive to the measurement of the Dicke narrowed Rayleigh peak and vibrational sidebands observed in cold atoms trapped in lattices.

In this paper we study the spectral profile of molecules trapped in deep one-dimensional (1D) optical lattices. In particular, we study the spectral profile of elastically scattered light along the axis of the lattice. We show that molecules trapped by short pulsed lattices in the 30 ns range will have a Dicke narrowed Rayleigh peak and vibrational sidebands with frequency shifts in the (100 MHz) range. We show that these spectral features will appear in room temperature gases up to pressures of 200 torr. Lastly, we explore the effect of adiabatic alignment of molecules in the lattice induced by the strong fields and calculate the effect of this process on the spectral features of trapped molecules.

II. THEORY

To calculate the spectra of trapped molecules we use the formalism detailed by Rautain and Sobelman [15], where the frequency dependence of the scattered light intensity is given by

$$I(\omega) = \frac{1}{\pi} \text{Re} \int_0^{\infty} e^{-i\omega t} \Phi(t) dt. \quad (1)$$

The function $\Phi(t)$ is the correlation amplitude of emitted radiation given by $\Phi(t) = \int d\mathbf{v} \int e^{-i\mathbf{k}\cdot\mathbf{r}} f(\mathbf{r}, \mathbf{v}, t) d\mathbf{r}$, where $f(\mathbf{r}, \mathbf{v}, t)$ is the molecular distribution function which varies in space (\mathbf{r}), velocity (\mathbf{v}), and time (t), and \mathbf{k} is the wave vector of the radiation.

The 1D molecular distribution function along the lattice direction x , is calculated from the Boltzmann kinetic equation with the periodic dipole force of the lattice \mathbf{F} . The Boltzmann equation is given by

$$\frac{\partial f}{\partial t} + \vec{v} \cdot \nabla f + \frac{\mathbf{F}}{M} \cdot \frac{\partial f}{\partial \mathbf{v}} = I_c, \quad (2)$$

where the interaction between the applied counterpropagating fields of intensity $I_1(t)$ and $I_2(t)$ leads to a 1D potential well, $U(x, t)$ [13], whose negative gradient yields a force

$$F(x, t) = -\frac{2\alpha\sqrt{I_1(t)I_2(t)}}{\epsilon_0 c} k \sin[2kx + \varphi_0]. \quad (3)$$

In this expression α is the effective polarizability, which has been shown to be well approximated by the static polarizability at the intensity and detuning from resonance considered here. The variable φ_0 is the initial phase and k is the magnitude of the wave vector.

Although there are radial and axial forces within a 1D lattice created by a typical Gaussian laser beam, we need only treat motion due to the larger axial forces along the direction defined here to be the x axis because we consider short pulsed fields of 30 ns duration [16]. To calculate the distribution function we use the initial condition $f(x, v, 0) = NW_M(v) \delta(x)$, which corresponds to the usual 1D Maxwell-Boltzmann distribution function for a gas in thermal equilibrium. The unperturbed gas density is given by N , and the normalized Maxwellian distribution function is defined as $W_M(v) = \frac{\exp(-Mv^2/2k_B T)}{(2\pi k_B T/M)^{1/2}}$. For the Dirac delta function $\delta(x)$ we use the continuous representation in the form $\delta(x, \Delta) = \frac{\exp[-(x/\Delta)^2]}{\Delta\pi^{1/2}}$, $\Delta \rightarrow 0$ [17]. The collisional integral has the form of $I_c = -\nu_c \{ [f(x, v, t) - W_M f(x, v', t)] dv' \}$, where ν_c is the collision frequency [15].

At a given initial phase φ_0 , the kinetic equation is solved at each spatial point x , and the result is averaged over the optical lattice wavelength $\lambda/2$, where λ is the wavelength of the radiation. The process is the same as averaging over all initial phases from 0 to 2π , where

$$I(\omega) = \frac{1}{2\pi} \int_0^{2\pi} I(\omega, \varphi_0) d\varphi_0. \quad (4)$$

We solve the 1D nonstationary Boltzmann equation (4) using the explicit second-order MacCormack method [18], apply-

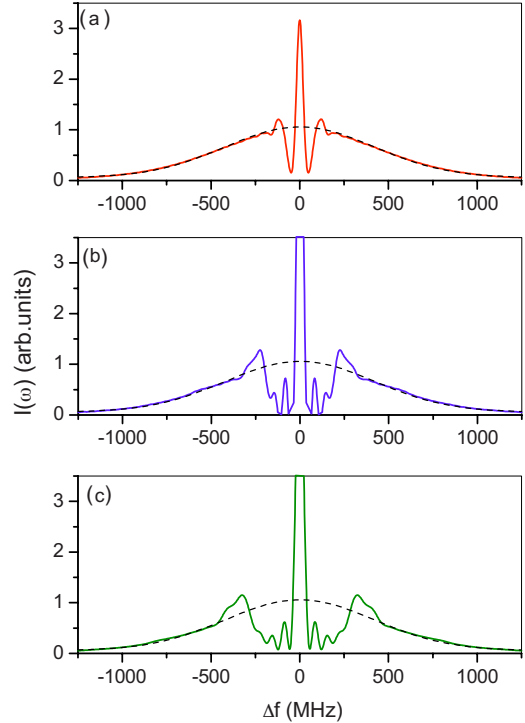


FIG. 1. (Color online) Spectral profiles of Rayleigh scattered light of molecules trapped in a pulsed optical lattice. The spectra of CO_2 gas for lattices with well depths $U/k_B = 15$ K (a), 78 K (b), and 157 K (c) are shown. The elastic Dicke narrowed peak and the near elastically scattered vibrational sidebands can be seen for a gas initially at a temperature of 295 K and a pressure of 5 torr. For reference, we also include the unperturbed spectra of the gas in each figure shown as the dashed line.

ing periodic boundary conditions over one lattice period. To reduce dispersive nonphysical ripples in this scheme, the 1D flux-corrected transport method was used [19]. This method was applied on each time step alternatively in the x and v directions.

III. SPECTRAL PROFILES

We apply the above formalism to the calculation of spontaneous Rayleigh scattering spectra of CO_2 gas along the lattice axis at room temperature (295 K) and a pressure of 5 torr along the direction of the lattice. We consider the situation where the gas is trapped and perturbed by a lattice produced by fields of constant intensity and duration of 30 ns. Such fields, with a near flat-top temporal profile, can be produced using commercially available pulsed laser systems using pulse slicing technology. The counterpropagating optical fields are at a wavelength of 532 nm producing lattice periods of 266 nm. The spectral profiles observed along the axis of the 1D lattice are shown in Fig. 1. For comparison, this figure also contains the 1D Gaussian spectral profile of the gas when no lattice field is applied (dashed line). The lattice spectra in Fig. 1 are calculated for optical well depths of $U/k_B = 15$ K, 78 K, and 157 K corresponding to equal lattice beam intensities of $2.5 \times 10^{15} \text{ W m}^{-2}$, $5.0 \times 10^{15} \text{ W m}^{-2}$ and $1.0 \times 10^{16} \text{ W m}^{-2}$, respectively. Each spectrum shows

the vibrational sidebands and the Dicke narrowed Rayleigh peaks, even though not all the gas is captured by the optical potential. The sidebands are shifted by approximately three orders of magnitude greater than observed in cold atom spectra, with the peak of the motional sidebands at ± 117 , ± 230 , and ± 326 MHz, respectively. The vibrational features are broader than the central Dicke narrowed peak due to the anharmonic nature of the lattice potentials. A maximum frequency shift of the sidebands can be estimated for molecules at the bottom of the well where it is approximately harmonic. The simple harmonic motion in this region produces a frequency shift given by

$$\nu = \pm \frac{k}{\pi} \sqrt{\frac{\alpha \sqrt{I_1 I_2}}{\epsilon_0 c M}}, \quad (5)$$

where M is the mass of the particle and all other variables are defined above. The maximum frequency shift determined from Eq. (5) for the three well depths is 144, 322, and 457 MHz and is in good agreement with the calculated spectral profiles of Fig. 1 where the motional sidebands begin to rise above the Doppler profile.

Although we have considered the classical motion of molecules in the lattice, the molecular motion will be quantized with the lowest vibrational states within the lattice separated by $\delta E = \hbar 2\pi\nu$. For the deepest lattice of well depth 157 K considered here energy levels are separated by $\delta E/k_B = 22$ mK. Due to the short interaction time (30 ns) and the high frequency of oscillation, such quantization should be measurable in a cold molecular beam where energy spreads of <100 mK can be achieved. For molecules seeded into these cold beams, the sidebands will become asymmetric revealing the quantized nature of the motion [7], providing that the population in the few occupied levels has a Boltzmann distribution. We also note that molecules trapped in these few states (vibrational levels) will be localized to within a few nanometers based on the spatial extent of the ground state wave function given by $[2\hbar/(M2\pi\nu)]^{1/2}$ [8], which corresponds to 1 nm for a well depth of 157 K.

The Rayleigh peak and the motional sidebands shown in Fig. 1 persist even at high pressures due to the relatively fast oscillations induced by the deep wells. This can be observed in Fig. 2, which are plots of the spontaneous scattering spectral profile of trapped CO₂ gas as a function of pressure from 5 torr to 100 torr at an initial temperature of 295 K for a fixed lattice well depth of 78 K. Figure 2 shows that the sidebands broaden with higher collision frequency due to the damping of the coherent oscillations within the lattice, while the height of the central peak reduces as collisions with untrapped molecules reduce the number of molecules trapped and localized by the lattice.

Since the polarizability-to-mass ratio can be used to uniquely identify a species [21], a measurement of the location of the sidebands in the Rayleigh scattering spectrum suggests a new approach to gas phase diagnostics. To illustrate this concept, spontaneous Rayleigh scattering spectra for xenon and carbon dioxide calculated using a lattice beam intensity of $5 \times 10^{15} \text{ W m}^{-2}$ are shown in Fig. 3. This intensity corresponds to a well depth of 78 K for CO₂ and 108 K

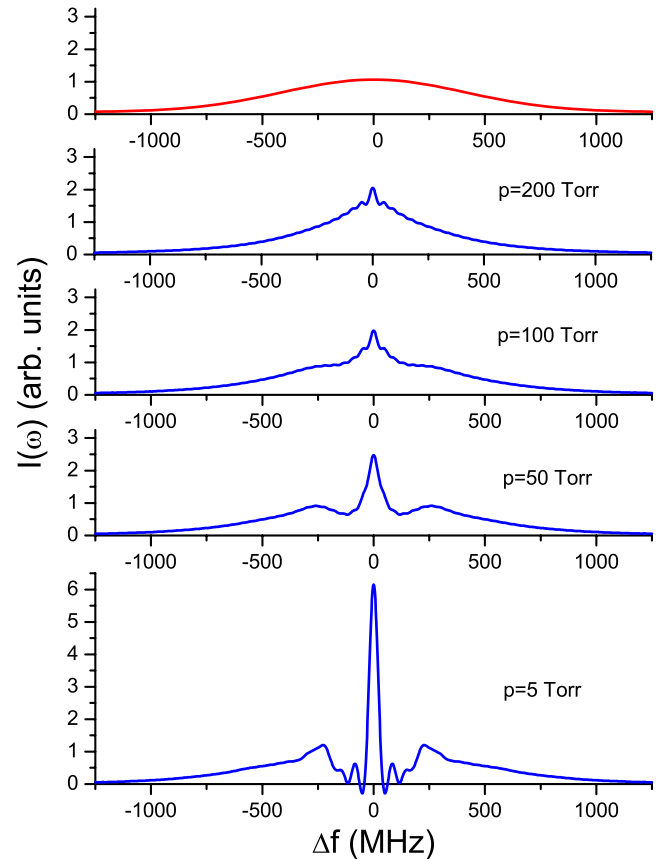


FIG. 2. (Color online) Spontaneous Rayleigh scattering spectra of CO₂ gas at 295 K in a lattice as a function of pressure from 5 torr to 200 torr for a well depth of 78 K. The graph at the top of the figure shows, for reference, the unperturbed Gaussian spectral profile. The sidebands and narrowed Rayleigh peak can be observed even when the collision frequency far exceeds the frequency shift of the sidebands and the average time between collisions is much less than the pulse duration of the fields.

for xenon. Although the xenon well depth is deeper due to a large polarizability of $4.5 \times 10^{-40} \text{ Cm}^2 \text{ V}^{-1}$ when compared to that of CO₂ ($3.2 \times 10^{-40} \text{ Cm}^2 \text{ V}^{-1}$), its Raman sidebands at 152 MHz have a smaller shift than CO₂ (226 MHz) be-

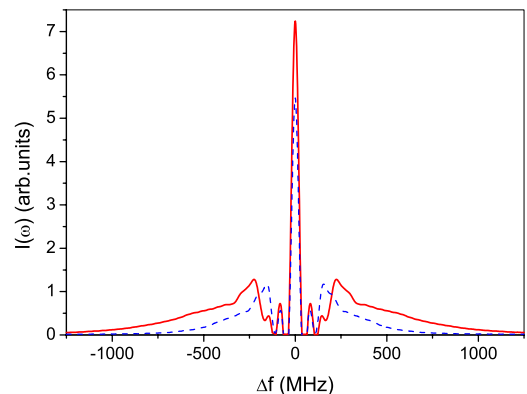


FIG. 3. (Color online) A comparison between the trapped spectral profile of CO₂ (solid line) and Xe gas (dashed line) at 295 K using lattice beam intensities of $5 \times 10^{15} \text{ W m}^{-2}$.

cause of its larger mass [Eq. (5)]. The maximum frequency of each sideband again corresponds well to that predicted by Eq. (5). It is clear that a mixture of species that do not collide over the duration of the laser pulse will produce separate vibrational sidebands that could be used to determine both the type of species by the frequency shift and the concentration by the height of each sideband. We note that because such high intensities are used, the gas pressure will be limited by optical breakdown to approximately several hundred torr.

All of the main spectral features calculated in Figs. 1–3 have been observed in the spectra of cold atoms, albeit at much smaller frequency scales. At higher intensities above 10^{15} W m^{-2} , and at low rotational temperatures, the field-induced alignment and the subsequent modification of the effective polarizability must be taken into account, a process that does not occur in atoms with a scalar polarizability. Molecular alignment changes the effective polarizability and thus the well depth and also the shape of the potential, ultimately leading to a modification in the spectral profile of molecules trapped in the lattice. At the intensities that we consider, almost complete alignment can be achieved in many cold molecular species. The alignment is characterized by the angle θ , between the symmetry axis of the molecule and the polarization vector of the field. In all linear molecules the symmetry axis, which is along the bond axis, is perpendicular to the angular momentum vector. The Hamiltonian for a linear molecule in a linearly polarized field reduces to [22]

$$H = B\mathbf{J}^2 - \frac{1}{2} \frac{I(x,t)}{\varepsilon_0 c} [\Delta\alpha \cos^2 \theta + \alpha_{\perp}], \quad (6)$$

where B is the rotation constant for the molecules, \mathbf{J} is the angular momentum operator, and $\Delta\alpha = \alpha_{\parallel} - \alpha_{\perp}$, where α_{\parallel} and α_{\perp} are the parallel and perpendicular polarizabilities with respect to the molecular symmetry axis. The expectation value of $\cos^2 \theta$ is determined by calculating the total rotational wave function of the molecule expressed as a superposition of field free eigenfunctions, whose coefficients are found by numerical solution of the Schrödinger equation [22]. To study this effect on the spontaneous Rayleigh scattering spectra we only consider adiabatic alignment by calculating the effective polarizability as a function of field intensity. This effective polarizability is used to modify the optical force [Eq. (3)]. The Boltzmann equation approach outlined above cannot be solved accurately when applied to the narrow velocity distribution of a 2 K molecular beam. To determine spectral profiles for this case we directly calculate the trajectories of a large range of particles subject to the periodic optical force of the lattice [Eq. (3)]. The particles are initially uniformly distributed over a lattice wavelength with a 1D thermal velocity distribution. The spectral profile of each particle is calculated via the approach of Galatry [20], where the spectral profile is given by Eq. (1) and the correlation function for each particle is given by $\Phi_c(t) = \int \exp\{-\frac{2\pi i}{\lambda}[x(t_0+t) - x(t_0)]\} dt_0$. The spectral profile for each particle is finally summed to determine the response of the ensemble. We have shown that the same results can be ob-

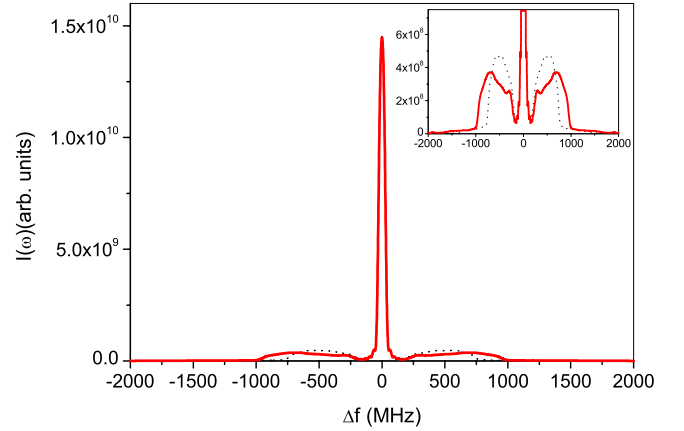


FIG. 4. (Color online) The spectral profile of CS_2 gas at 2 K trapped in optical lattice utilizing the average polarizability and the intensity dependent polarizability due to field-induced alignment of the molecules. Both spectra are calculated using lattice beam intensities of $1 \times 10^{16} \text{ W m}^{-2}$. The dashed line represents the spectral profile calculated using the average polarizability and the solid line due to the intensity dependent polarizability. In both cases the Dicke narrowed peak is the dominant spectral feature. The inset is a graph with an expanded vertical axis of the main figure, which shows the difference between the vibrational sidebands of the lattice for the two cases.

tained from the correlation function determined by solution of the Boltzmann equation where few collisions occur during the lattice pulse. Figure 4 contains the Rayleigh spectra calculated for CS_2 with this intensity dependent effective polarizability using the Galatry formalism using lattice beam intensities of $1 \times 10^{16} \text{ W/m}^2$. For comparison, we also show the spectrum obtained using the average value of the polarizability of $\alpha_{eff} = 9.7 \times 10^{-40} \text{ Cm}^2 \text{ V}^{-1}$. Both spectral profiles show broad motional sidebands for both the average and intensity dependent polarizability with the peak of each case at 526 and 708 MHz from the central Rayleigh peak. The much larger frequency shift and width of the sidebands, when the intensity dependent polarizability is used, is due to the larger maximum well depth of 427 K compared with 264 K for the averaged polarizability. The intensity dependent polarizability also leads to an increased anharmonicity in the lattice potential as it is no longer purely sinusoidal. For frequency shifts in the motional sidebands of less than 304 MHz, the line shapes for both the constant and intensity dependent polarizability is the same. This occurs because the intensity dependent polarizability is approximately equal to the average polarizability in the low intensity regions of the lattice where the force on the molecules is relatively weak. However, near the antinodes of the interference pattern where the intensity is near its maximum, the molecule aligns and the effective force and thus oscillation frequency is larger. This is observed in the spectra of the sidebands for frequency shifts greater than 304 MHz where the line shapes for each case diverge.

IV. CONCLUSIONS

We have presented calculations of the spontaneous Rayleigh scattering spectrum for room temperature and cold (2

K) molecules trapped in deep optical lattices. These calculations have been based on realistic experimental parameters that have been used for slowing molecules in molecular beams and for four-wave mixing measurements using coherent Rayleigh scattering. By using fields that are several orders of magnitude greater than that used in cold experiments, we have shown that the same spectral features should be observed over much shorter time scales (30 ns) with motional sidebands shifted by up to 700 MHz. We have shown that the large oscillation frequency within the wells means that the sidebands can be observed at even relatively high pressures, suggesting that this phenomena could be used as a nonresonant technique for measurement of species type and concentration. In addition, the Dicke narrowed peaks could

be used for high-resolution molecular gas phase spectroscopy at room temperature up to pressures in the 100 torr range. The large oscillation frequency also implies that quantized motion within the potential could be observed in a cold molecular beam. As the oscillation frequency is proportional to the square root of the polarizability-to-mass ratio and this value does not change by more than an order of magnitude for any polarizable particle, these spectral features could, in principle, be observed in more massive molecules and particles. Finally, we have explored the effect of the intensity dependent polarizability induced by molecular alignment of CS₂ and show that the anharmonicity and the deeper well depth are manifested in the motional sidebands of the spectral profile of the trapped gas.

-
- [1] R. H. Dicke, Phys. Rev. **89**, 472 (1953).
 [2] E. C. Beaty, P. L. Bender, and A. R. Chi, Phys. Rev. **112**, 450 (1958).
 [3] S. Nazemi, A. Javan, and A. S. Pine, J. Chem. Phys. **78**, 4797 (1983).
 [4] R. H. Romer and R. H. Dicke, Phys. Rev. **99**, 532 (1955).
 [5] R. L. Mössbauer, Z. Phys. **151**, 124 (1958).
 [6] V. S. Letokhov and B. D. Pavlik, Appl. Phys. (Berlin) **9**, 229 (1976).
 [7] P. S. Jessen, C. Gerz, P. D. Lett, W. D. Phillips, S. L. Rolston, R. J. C. Spreeuw, and C. I. Westbrook, Phys. Rev. Lett. **69**, 49 (1992).
 [8] P. Verkerk, B. Lounis, C. Salomon, C. Cohen-Tannoudji, J.-Y. Courtois, and G. Grynberg, Phys. Rev. Lett. **68**, 3861 (1992).
 [9] J. C. Bergquist, W. M. Itano, and D. J. Wineland, Phys. Rev. A **36**, 428 (1987).
 [10] G. Grynberg, B. Lounis, P. Verkerk, J.-Y. Courtois, and C. Salomon, Phys. Rev. Lett. **70**, 2249 (1993).
 [11] G. Birkl, M. Gatzke, I. H. Deutsch, S. L. Rolston, and W. D. Phillips, Phys. Rev. Lett. **75**, 2823 (1995).
 [12] D. J. Wineland and H. Dehmelt, Bull. Am. Phys. Soc. **20**, 637 (1975).
 [13] R. Fulton, A. I. Bishop, M. N. Shneider, and P. F. Barker, Nat. Phys. **2**, 465 (2006).
 [14] H. T. Bookey, M. N. Shneider, and P. F. Barker, Phys. Rev. Lett. **99**, 133001 (2007).
 [15] S. G. Rautian and I. I. Sobelman, Sov. Phys. Usp. **9**, 701 (1967).
 [16] G. Dong, W. Lu, and P. F. Barker, Phys. Rev. E **68**, 016607 (2003).
 [17] G. A. Korn and T. M. Korn, *Mathematical Handbook for Scientists and Engineers; Definitions, Theorems, and Formulas for Reference and Review*, 2nd ed. (McGraw-Hill, New York, 1968).
 [18] J.D Anderson, Jr., *Computational Fluid Dynamics* (McGraw-Hill, New York, 1995).
 [19] J. P. Boris and D. L. Book, J. Comput. Phys. **20**, 397 (1976).
 [20] L. Galatry, Phys. Rev. **122**, 1218 (1961).
 [21] B. S. Zhao *et al.*, Phys. Rev. Lett. **85**, 2705 (2000).
 [22] T. Seideman, J. Chem. Phys. **107**, 10420 (1997).